

In Silico Screening of Natural Metabolites as Inhibitors of Biosynthesis and Transport of Enterobactin

Joseph Christina Rosy ¹, Haribalaganesh Ravinarayanan ², Palaniappan Gokila ¹, Thirumudikari Navamuthamani ¹, Shakti Chandra Vadhana Marimuthu ¹, Selvaraj Kunjiappan ¹, Krishnan Sundar ^{1,*}

¹ Department of Biotechnology, School of Bio and Chemical Engineering, Kalasalingam Academy of Research and Education, Krishnankoil, Tamilnadu, India

² Department of Ocular Pharmacology, Aravind Medical Research Foundation, Madurai, Tamilnadu, India

* Correspondence: sundarkr@klu.ac.in (K.S.);

Scopus Author ID 7003264215

Received: 21.12.2021; Accepted: 15.01.2022; Published: 25.03.2022

Abstract: As antibiotic resistance is becoming a more serious issue, eliminating essential nutrients from the microenvironment of pathogens, thereby diminishing their growth, would be an effective alternative to widely used antibiotics. Inhibition of iron sequestration in bacteria is one of the alternative antibacterial strategies. As bacteria use siderophores, small molecules that chelate iron from host proteins for iron sequestration, inhibition of siderophore biosynthesis and transport would be a promising way of finding an alternative to the antibiotics. The objective of the current work was to screen for natural metabolites as potential binders of selected drug targets involved in iron acquisition in *E. coli*. Isochorismate synthase (ICS), an enzyme involved in siderophore biosynthesis, enterobactin, and a membrane protein FepA transports enterobactin-Fe complex into bacterial cells, were chosen as drug targets. Forty-three marine metabolites and 87 plant metabolites were screened *in silico*, as inhibitors for the selected drug targets. Three marine metabolites viz. Plakorstatin B (-8.76) laurenditerpenol (-8.44), isogranulatimide (-8.39) and, and two plant metabolites: quercetin (-7.97) from *Withania somnifera* and vomifoliol (-7.96) from *Morinda citrifolia* were the top-binders for ICS, and further analysis indicated that these compounds interact with the same amino acids that are interacting with the natural ligand of ICS. Withanolide D (-12.61) from *W. somnifera*, rubiadin (-12.25), and daucosterol (-11.87) from *M. citrifolia*, and two marine metabolites: bistramide A (-11.8) and isogeoditin A (-11.56) were found to be the top-binders for FepA. These compounds could act as lead molecules for the design and development of effective siderophore inhibitors, thereby controlling the growth of microbial pathogens.

Keywords: iron-sequestration; siderophore; enterobactin; isochorismate synthase; FepA.

© 2022 by the authors. This article is an open-access article distributed under the terms and conditions of the Creative Commons Attribution (CC BY) license (<https://creativecommons.org/licenses/by/4.0/>).

1. Introduction

Host-microbe interaction is a never-ending hide-and-peek game. Though the host has been evolving with novel defense mechanisms, the same way, microorganisms have been evolving with strategies to become resistant to antibiotics. Antibiotic resistance is developed by various means such as selection, mutation, and transduction, while microbial resistance can either be inherent in the organism or acquired through the environment [1]. According to WHO, infections caused by resistant microorganisms often fail to respond to treatment, resulting in prolonged illness and death risk [2]. The current understanding of bacterial pathogenesis has

uncovered many potential approaches to develop novel drugs which are alternatives to antibiotics. As these alternative drugs disarm the pathogen rather than kill or halt pathogen growth, it has been hypothesized that they will generate a much weaker selection for resistance than traditional antibiotics [3]. Inhibition of iron transport in bacteria is considered as one of the important alternative approaches to control bacterial infections [4]. Most organisms require iron as an essential element for various metabolic pathways. Most of the iron in the biological fluids of vertebrates is bound by transferrin, lactoferrin, and hemoglobin [5]. Therefore, microorganisms depend heavily on their ability to use the host-complexed iron in establishing an infection. A key feature that enables pathogenic bacteria to survive within the vertebrate host is the production of siderophores, a group of small molecular weight iron-sequestering compounds, and the synthesis of their cognate transport systems, which are crucial in overcoming the non-specific defense mechanisms of the host and allow for bacterial multiplication [6, 7]. Therefore, inhibition of siderophore biosynthesis in bacterial pathogens is considered an innovative approach to design drugs to treat bacterial infections [8-10].

Enterobactin is a high-affinity siderophore that acquires iron for microbial systems. It is primarily present in Gram-negative bacteria, such as *Escherichia coli* and *Salmonella typhimurium* [11, 12]. The biosynthesis and mechanism of transport of iron by enterobactin were well studied and reported by many researchers [13, 14]. An enzyme isochorismate synthase (ICS) [15] involved in the biosynthesis of enterobactin and a membrane protein FepA [16], which is involved in the active transport of ferric-enterobactin complex from the extracellular space into the periplasm of Gram-negative bacteria, were chosen as drug targets for this study. Inhibition of these target proteins may cease the survival and virulence of bacterial pathogens, which exclusively use enterobactin as iron chelators. In this study, a set of marine and plant-derived metabolites were screened *in silico* as inhibitors of ICS and FepA. The active compounds with a high binding affinity towards these targets can be purified and further studied as enterobactin biosynthesis and transport inhibitors.

2. Materials and Methods

2.1. Materials.

The crystal structures of the two proteins, isochorismate synthase (ICS; PDB ID: 3HWO) and FepA (PDB ID: 1FEP), were downloaded from Protein Data Bank (PDB). The features of the two proteins are presented in Table 1. A total of 43 marine compounds selected from the literature was used for screening. In addition, compounds from three plants, namely *Justicia adhatoda*, *Withania somnifera*, and *Morinda citrifolia* were also selected from Dr. Dukes Phytochemical and Ethnobotanical Databases [17]. The above three plants were chosen for the study as the active compounds of these plants were least explored for various biological activities. A total of 130 compounds were selected for this study. All these compounds were downloaded from the Chempidder database.

Table 1. Features of the selected drug targets.

Features	FepA	Isochorismate Synthase
PDB ID	1FEP	3HWO
Experimental Technique	X-Ray diffraction	X-Ray diffraction
Resolution	2.4Å	2.30Å
Source Organism	<i>E. coli</i>	<i>E. coli</i>
Length	724 amino acids	394 amino acids

Features	FepA	Isochorismate Synthase
Natural Ligand	Not available	(5S,6S)-5-[(1-carboxyethenyl)oxy]-6-hydroxycyclohexa-1,3-diene-1-carboxylic acid

2.2. Homology search.

The selected proteins, FepA and ICS, were searched against human proteome for homologous proteins using protein BLAST. This was to ensure that the drug targets do not share homology with any of the human proteins so that targeting them will not cause any side effects.

2.3. Protein and ligand preparation.

Computer System with 2x Intel® Core™ Duo, 2.53 GHz processor, 4GB RAM, and Ubuntu 12.10 operating system was used for carrying out molecular docking studies. AutoDock 4.2 was used for molecular docking, and Discovery Studio Client 4.0 was used for the visualization of protein-ligand interactions.

The proteins and ligands were prepared for docking using the graphical user interface of AutoDockTools. The preparation involved adding all hydrogen atoms to the proteins, which is necessary for calculating partial atomic charges. Water molecules and heteroatoms were removed from the protein molecule. The natural ligand for ICS, isochorismate, was also used for docking.

2.4. Grid calculation and docking.

A three-dimensional grid box was generated to embed the protein, and grid parameters were set. Grid maps were calculated by running AutoGrid 4, which was then used by AutoDock for docking calculations. Docking parameters were set by the docking wizard of AutoDockTools as described earlier [18]. Conformation search was performed by Lamarckian Genetic Algorithm for 100 cycles [19]. AutoDock 4 uses the pre-calculated grid maps to calculate the interaction energies of ligands with the proteins. The binding energies for each conformation of the ligand with the proteins were determined by running AutoDock 4 [20].

2.5. Analysis of docking results.

Analysis of docking was performed by using the graphical user interface of AutoDockTools and Discovery Studio Client 4.0. The binding energies of each conformation of docked compounds were calculated. Various types of interactions between ligand and receptor such as hydrogen bonds, hydrophobic interactions, van der Waals and electrostatic interactions were visualized using Discovery Studio. AutoDock calculates the binding energy by an energy function derived from molecular mechanics terms such as van der Waals energy, hydrogen bond energy, torsional energy, electrostatic energy, and desolvation energy.

2.6. Analysis of pharmacokinetic and physicochemical parameters.

The ADME properties such as the molecular weight, solubility, bioavailability, brain penetration, and gastrointestinal absorption of the top 5 binders were predicted using SwissADME. The toxicity of the top-binding metabolites was predicted using ToxiM. The bioactivity of the lead compounds was predicted using Way2Drug/PASS, a QSAR based

bioactivity prediction server. The general antibacterial activity was considered as the bioactivity of the compound. Compounds with the probability of bioactivity (P_a) > 0.3 and the probability of inactivity (P_i) < 0.05 were considered as promising drug candidates [21].

3. Results

3.1. Homology search.

To ensure no similarity exists between the target proteins and the human proteins, the sequences of FepA and ICS were downloaded and searched against the human genome using the BLASTx program. The results indicated that none of the human proteins shared similarities with the selected drug targets.

3.2. Molecular docking studies.

A total of 130 natural compounds of marine and plant origin were selected and docked with the ligand-binding site of FepA and ICS to find their interaction as FepA and ICS binders. The binding energies of compounds docked with FepA and ICS are listed in Table 2.

Table 2. Binding energies of compounds docked with FepA and Isochorismate synthase.

S. No	Ligand	Binding Energy (kcal/mol)	
		FepA	ICS
I	Natural Ligand	NA	-8.72
Marine Natural Compounds (Source)			
1.	Actinomadura Xanthone (Marine Actinomycete)	-7.32	-6.92
2.	Amphidinolide C (algae)	13.07	1580
3.	Amphidinolide X (algae)	-7.69	62.04
4.	Andavadoic acid (Sponge)	-8.63	-2.73
5.	Aplysinopsin (sponges, corals, sea anemone)	-7.76	-7.34
6.	Bistramide A (Ascidian)	-11.8	491.41
7.	Carotene (Microalgae)	-11.02	NA
8.	Certonardosterol A2 (Starfish)	-11.26	78.93
9.	Certonardosterol C2 (Starfish)	-10.33	26.69
10.	Certonardosterol D (Starfish)	-11.19	18.79
11.	Certonardosterol D2 (Starfish)	-9.68	20.46
12.	Certonardosterol D3 (Starfish)	-10.17	25.5
13.	Certonardosterol E2 (Starfish)	-10.08	43.7
14.	Certonardosterol E3 (Starfish)	-10.51	23.67
15.	Certonardosterol N1 (Starfish)	-9.86	34.81
16.	Certonardosterol Q6 (Starfish)	-9.46	14.61
17.	Cibrostatin 6 (Sponge)	-7.22	-6.32
18.	Cytonic acid A (Cytonaema sp)	-9.93	NA
19.	Cytonic acid B (Cytonaema sp)	-9.3	NA
20.	Discorhabdin L (Sponge)	-8.02	-5.49
21.	Dolastatin 11 (Mollusc)	1.13	10100
22.	Dolastatin 15 (Mollusc)	1.48	1070
23.	Iriciniastatin A (Sponge)	-9.45	116.06
24.	Isogeoditin A (Sponge)	-11.56	76.85
25.	Isogeoditin B (Sponge)	-11.23	160.86
26.	Isogranulatimide (Ascidian)	-8.68	-8.39
27.	Jaspine B (sponge)	-7.41	-4.87
28.	Lamellarin D (algae)	-6.46	106.72
29.	Laurenditerpenol (marine algae)	-9.01	-8.44
30.	Lissoclinolide (Ascidian)	-7.42	-7.48
31.	Microcionamide A (Sponge)	82.81	1470
32.	Microcionamide B (Sponge)	45.7	952.8
33.	Mycalazal 8 (Sponge)	-6.25	5.48
34.	Neoamphimedine (Sponge)	-9.08	-0.7
35.	Neohalichondramide (Sponge)	17.03	877.85

S. No	Ligand	Binding Energy (kcal/mol)	
		FepA	ICS
36.	Ophiobolin A (Fungus)	-10.11	38.8
37.	Peloruside A (Sponge)	-8.9	86.62
38.	Phakellistatin 1(Sponge)	-	320.47
39.	Plakinamine K (Sponge)	-	87.87
40.	Plakorstatin A (Sponge)	-	-6.83
41.	Plakorstatin B (Sponge)	-8.4	-8.76
42.	Reineramycin J (Sponge)	-6.3	240.54
43.	Tasiamide B (bacteria)	65.23	1460
Compounds from <i>J. adhatoda</i>			
1	2',4'-Dihydroxychalcone-4-glucoside	-10.1	6.55
2	Adhatodine	-8.44	-2.11
3	Anisotine	-8.4	3.53
4	Arachidic acid	-6.96	-5.27
5	Behenic acid	-7.89	-0.99
6	Betaine	-3.55	-4.14
7	Beta-Sitosterol	-	-
8	Beta-Sitosterol-Beta-D-glucoside	-	-
9	Deoxyvascinone	-6.7	-6.29
10	Lignocericacid	-7.31	4.29
11	Linoleicacid	-7.44	-5.03
12	Oleicacid	-7	-6.1
13	Oscine	-5.3	-4.75
14	Peganine	-6.58	-7.08
15	RAA	-6.6	16.69
16	Vasicine	-6.75	-6.87
17	Vasicinol	-7.36	-7.84
18	Vasicinone	-6.73	-6.46
19	Vasicoline	-6.45	-6.65
20	Vasicolinone	-7.67	-2.19
Compounds from <i>W. somnifera</i>			
1	2,3 Dehydrosomnifericin	-10.65	52.93
2	2,3 Dihydrowithaferin	-9.95	61.16
3	Bellaradine	-6.57	-5.14
4	Campesterol	-10.04	2.73
5	Daucosterol	-11.87	271.14
6	D-Galactitol	-6.58	-5.8
7	Hydroxyproline	-5.35	-5.27
8	Isopelletierine	-4.53	-5.45
9	N-Hentriacontane	-5.51	44.38
10	Pseudotropine	-	-5.06
11	Quercetin	-9.47	-7.97
12	Quinicacid	-7.25	-6.74
13	Quresimine A	-11.27	74.58
14	Scopoletin	-6.49	-6.5
15	Sominone	-11.4	12.78
16	Tropanol	-5.31	-5.05
17	Withanolide D	-12.61	87.17
18	Withanolide F	-11.34	35.66
19	Withanolide L	-10.59	37.5
20	Withanone	-11.39	38.77
Compounds from <i>M. citrifolia</i>			
1	2-Ethylhexanoate	-5.55	-6.26
2	2-Heptanone	-4.38	-4.61
3	2-Methyl butanoic acid	-5.06	-5.37
4	2-Methyl hexanoate	-5.29	-6.28
5	2-Methyl propanoic acid	-4.72	-5.19
6	8,11,14-eicosatrienoic acid	-6.89	-5.92
7	Acetoin	-4.18	-4.44
8	Adipic acid	-6.64	-5.72
9	Alizarin	-7.98	-7.58
10	Alkamid	-4.6	-4.01
11	Asperulosidic acid	-9.7	-6.69
12	Benzoic acid	-5.47	-6.43
13	Benzylalcohol	-4.82	-4.6
14	Biochanin A	-8.61	-6.01

S. No	Ligand	Binding Energy (kcal/mol)	
		FepA	ICS
15	Butyric acid	-4.39	-5.03
16	Damnacanthal	-7.96	-6.93
17	Deacetylasperulositic acid	-10.45	-5.03
18	Elaidic acid	-6.7	-5.15
19	Ethylcaprylate	-	-5.56
20	Ethyldecanoate	-6.13	-7.27
21	Ethylpalmitate	-5.3	-5.29
22	Eugenol	-5.77	-6.51
23	Gentisic acid	-7.33	-7.17
24	Heptanoic acid	-4.91	-5.7
25	Hexanoic acid	-4.92	-5.86
26	Linoleic acid	-7.38	-6.54
27	Lucidin	-8.27	-7.54
28	Methyl decanoate	-5.1	-5.72
29	Methyl elaidate	-5.36	-4.34
30	Methyl octanoate	-5.45	-5.4
31	Methyl oelate	-7.59	-6.01
32	Methyl palmitate	-5.37	-5.88
33	Morindone	-	Error
34	Myristic acid	-6.92	-6.65
35	Niacin	-5.71	-6.05
36	Nonanoic acid	-5.42	-6.21
37	Nordamnacanthal	-7.4	-6.91
38	Octanoic acid	-5.19	-6.05
39	Phycion	-8.41	-5.23
40	Prenol	-4.21	-4.08
41	Rubiadin	-12.25	30.13
42	Rubichloric acid	-9.63	-6.9
43	Thiamin	-	Error
44	Undecanoic acid	-	-6.6
45	Ursolic acid	-	91.66
46	Vomifoliol	-7.92	-7.96
47	(Z)-6-Dodeceno-gamma-lactone	-6.11	-6.67

In total, 43 marine compounds have been docked with FepA, out of which 33 compounds were found to be interacting with FepA. Eleven of these compounds exhibited higher binding with less than -10 kcal/mol binding energies. The top binder was bistramide A with a binding energy of -11.8 kcal/mol followed by isogeoditin A (-11.56 kcal/mol).

Twenty compounds from *J. adhatoda*, 20 from *W. somnifera* and 47 from *M. citrifolia* were docked against FepA, out of which 18, 19, and 42 compounds, respectively, were found to be interacting with FepA. The top five binders were withanolide D (binding energy of -12.61), rubiadin (-12.25), daucosterol (-11.87), bistramide A (-11.8). Of these, withanolide D and daucosterol are from *W. somnifera*, rubiadin is from *M. citrifolia*, and bistramide A and isogeoditin A are from marine ascidian and sponges respectively. The top binders, their source, and binding energies are listed in Table 3. The amino acids of FepA, which interact with their top 5 binders, are presented in Figure 1. The amino acid residues Lys47, Leu57, Arg70, Arg108, Arg225, and Pro712 were found to be common in all the interactions. Interestingly, Lys47 and Pro712 are the common amino acids interacting with all five compounds.

Table 3. Top five binders of FepA.

S. No	Ligand	Source	Binding Energy (kcal/mol)
1	Withanolide D	<i>W. somnifera</i>	-12.61
2	Rubiadin	<i>M. citrifolia</i>	-12.25
3	Daucosterol	<i>M. citrifolia</i>	-11.87
4	Bistramide A	Marine ascidian	-11.8
5	Isogeoditin A	Marine sponge	-11.56

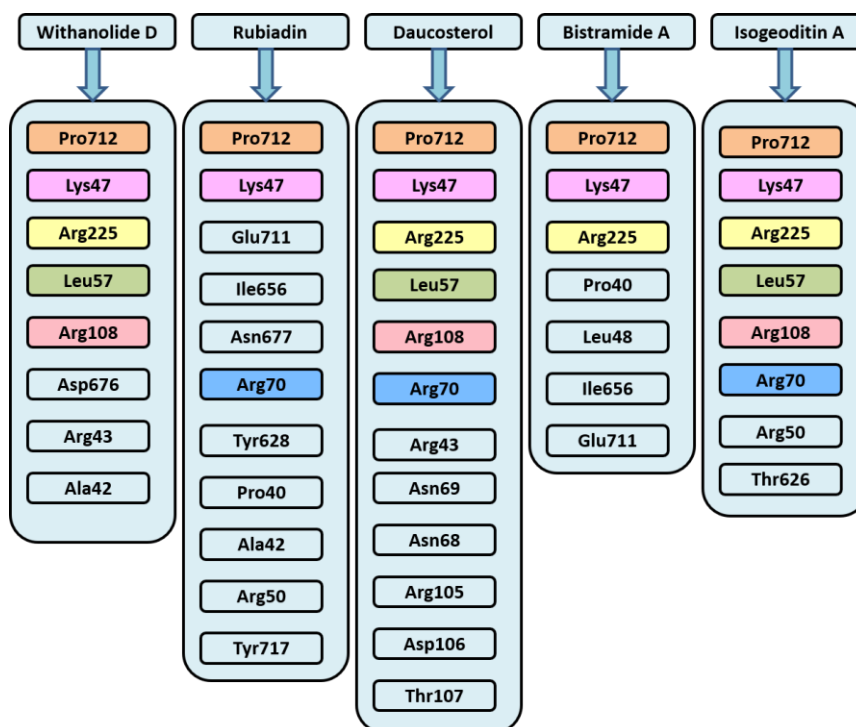


Figure 1. Amino acids of FepA are involved in interaction with the top five binders.

The residues Lys47, Leu57, Arg70, Arg108, Arg225, and Pro712, are found to be common in all the interactions. Among them, Lys47 and Pro712 are found to be interacting with all five compounds.

Out of the 43 marine compounds tested, only 12 were found to be interacting with ICS. Eight of these compounds exhibited less than -6 kcal/mol binding energy. Similarly, 14 out of 20 compounds from *J. adhatoda* were found to be interacting with ICS, whereas only 9 compounds out of 20 from *W. somnifera* and 44 out of 47 compounds from *M. citrifolia* were interacting with ICS. Plakorstatin B, laurenditerpenol, isogranulatimide, quercetin, and vomifoliol were the top 5 binders of ICS; their source and binding energies are listed in Table 4. The amino acids of ICS which interact with their top 5 binders are presented in Figure 2. The natural ligand present in the crystal structure of ICS, (5S,6S)-5-[(1-carboxyethenyl)oxy]-6-hydroxycyclohexa-1,3-diene-1-carboxylic acid (isochorismate) was also docked with isochorismate synthase, and it was found to be interacting with ICS with the binding energy of -8.72 Kcal/mol.

Table 4. Top five binders of isochorismate synthase.

Ligand name	Source	Binding energy (kcal/mol)
Plakorstatin B	Marine sponge	-8.76
Laurenditerpenol	Marine algae	-8.44
Isogranulatimide	Marine ascidian	-8.39
Quercetin	<i>W. somnifera</i>	-7.97
Vomifoliol	<i>M. citrifolia</i>	-7.96

The interaction of withanolide D with FepA and interaction of plakorstatin B with ICS are depicted in Figures 3 and 4, respectively. Withanolide D was found to fit inside the β -barrel structure of FepA (Figure 5). Plakorstatin B, the top most binder of ICS interacts with almost all the amino acids in the active site. Plakorstatin B interacts with amino acids that are exactly interacting with the natural ligand present in the crystal structure of ICS (Figures 2, 4, 6). The alignment of the docked pose of plakorstatin B with the natural ligand is shown in Figures 7a and 7b.

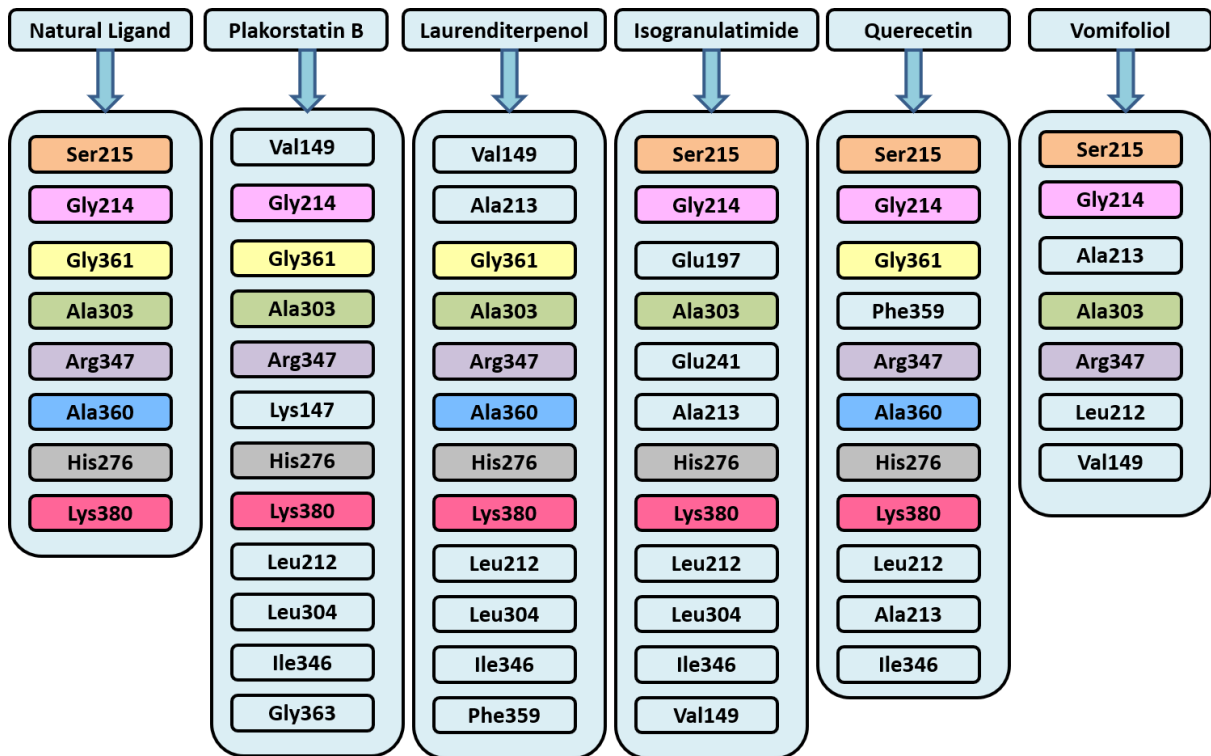


Figure 2. Amino acids of Isochorismate synthase involved in interaction with the top five binders. The highlighted amino acids (Ser215, Gly214, Gly361, Ala303, Arg347, Ala360, His276, and Lys380) are found to be interacting with the self-ligand present in the crystal structure and also with these top five binders. The maximum interaction with the active site amino acids was found in the compound plakorstatin B.

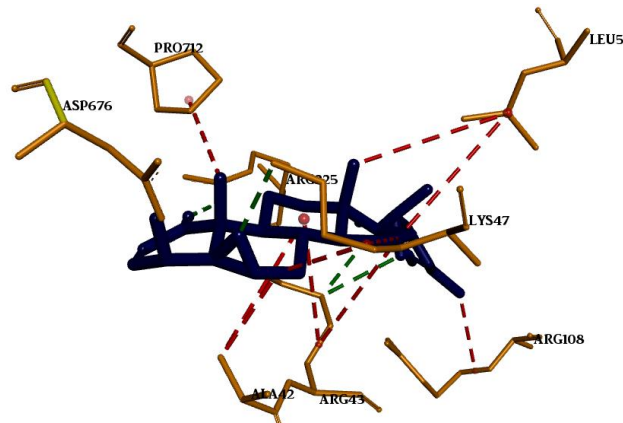


Figure 3. Interaction of withanolide D with FepA (Green color indicates hydrogen bonds; Red color indicates hydrophobic interactions).

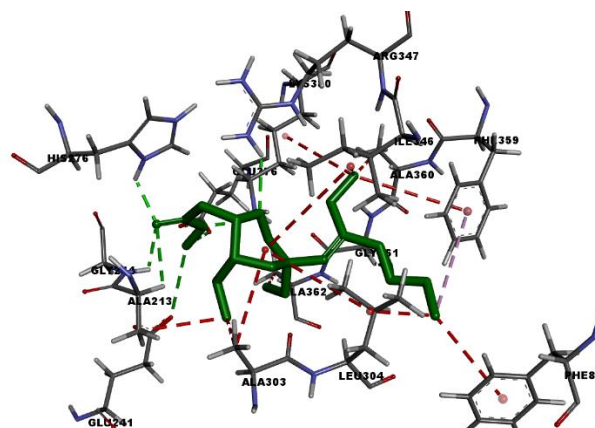


Figure 4. Interaction of plakorstatin B with ICS (Green color indicates hydrogen bonds; Red denotes hydrophobic interactions).

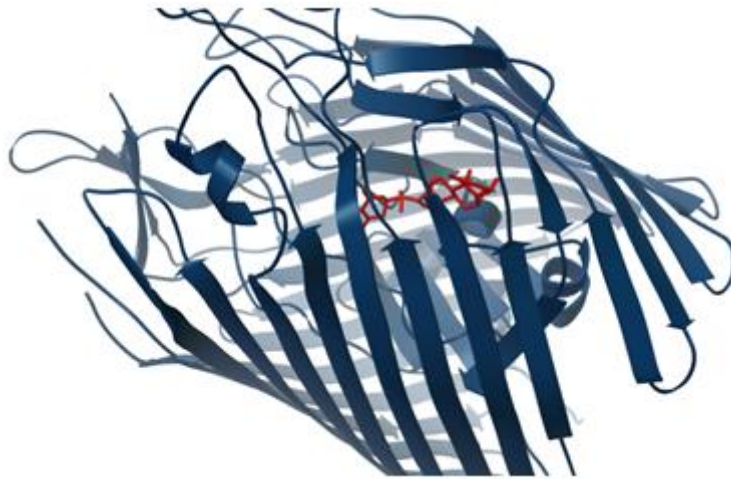


Figure 5. Binding of withanolide D inside the β -barrel structure of Fep A.

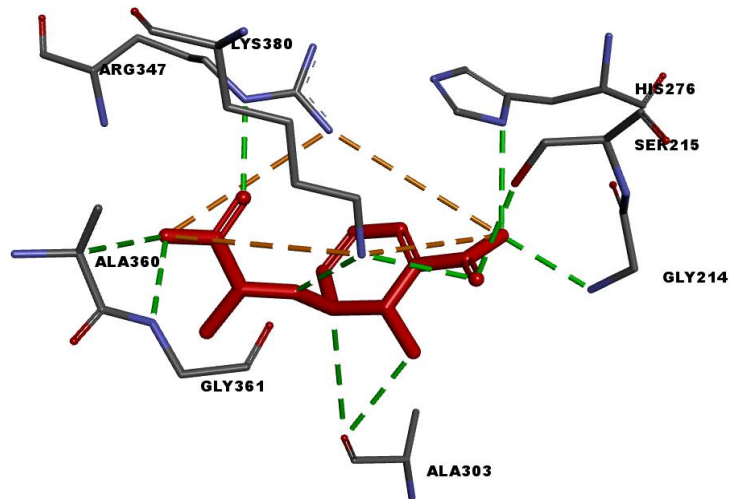


Figure 6. Interaction of natural ligand ((5S,6S)-5-[(1-carboxyethenyl)oxy]-6-hydroxycyclohexa-1,3-diene-1-carboxylic acid) with ICS (Green color indicates hydrogen bonds; Orange indicates hydrophobic interactions).

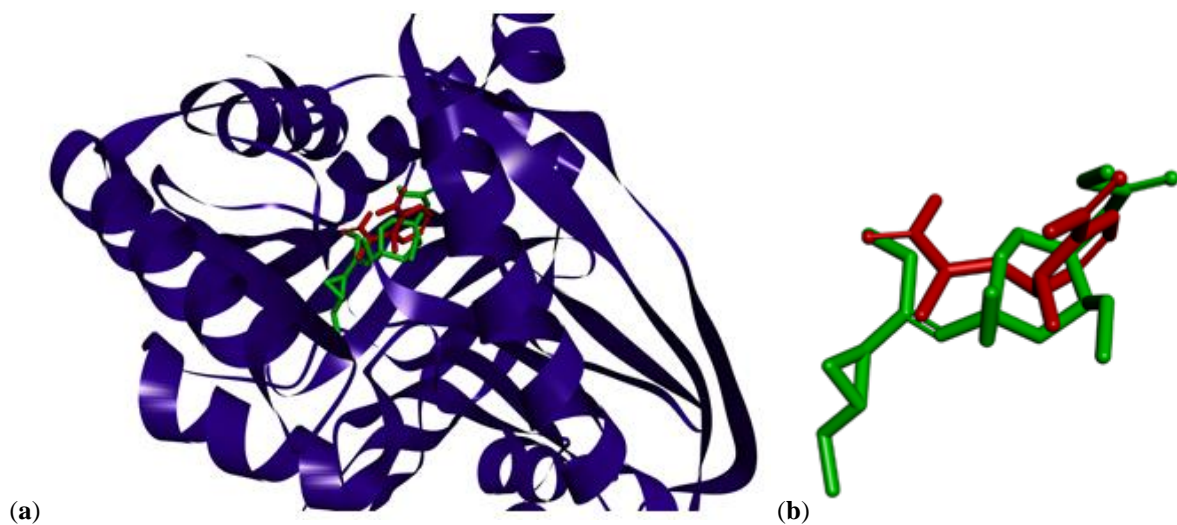


Figure 7. (a) Alignment of docked conformation of plakorstatin B with the natural ligand in the active site of ICS (Red color indicates Natural ligand and Green is Plakorstatin B); (b) Alignment of docked conformation of plakorstatin B with the natural ligand (Red color indicates Natural ligand and Green indicates Plakorstatin B).

The ADME/T analysis of the top binders of Fep A and ICS are presented in Tables 5 and 6, respectively. Among the top 5 binders of FebA, two of the compounds, Daucoesterol and Bistramide A, exhibited a single violation in the Lipinski's rule, whereas no violations were found in other compounds. This is because both compounds had a molecular weight of more than 500. Whereas no violations were found in all the top binders of ICS. The QSAR based prediction of antibacterial activity of the top, binding compounds was performed, and all the top binders of ICS and FepA, except Vomifoliol and Isogranulatimide, were found to show $P_a > 0.3$ and $P_i < 0.05$, which indicates that these compounds are eligible for being studied further as drug candidates.

Table 5. ADME/T Analysis of Top Binders of FepA.

	Withanolide D	Rubiadin	Daucoesterol	Bistramide A	Isogeotidin A
Molecular weight (g/mol)	470.60	254.24	576.85	704.98	450.61
Number of heavy atoms	34	19	41	50	33
Number of aromatic heavy atoms	0	12	0	0	0
Number of rotatable bonds	2	0	2	20	5
Number of H-bond acceptors	6	4	6	8	4
Number of H-bond donors	2	2	4	4	0
Log $P_{o/w}$	3.35	2.23	5.51	5.12	5.12
Lipinski Rule of Fives	0 violation	0 violation	1 Violation; mol wt >500	1 Violation; mol wt >500	0 violation
Bioavailability Score	0.55	0.55	0.55	0.55	0.55
GI absorption	High	High	Low	Low	High
BBB permeant	No	Yes	No	No	No

GI- Gastro Intestinal; BBB- Blood-Brain Barrier.

Table 6. ADME/T Analysis of Top Binders of ICS.

	Plakorstatin B	Laurenditerp enol	Isogranulati mide	Quercetin	Vomifoliol
Molecular weight (g/mol)	340.45	306.48	276.25	302.24	224.30
Number of heavy atoms	24	22	21	22	16
Number of aromatic heavy atoms	0	0	19	16	0
Number of rotatable bonds	9	4	0	1	2
Number of H-bond acceptors	5	2	4	7	3
Number of H-bond donors	0	1	2	5	2
Log $P_{o/w}$	3.70	4.23	1.47	1.23	1.53
Lipinski Rule of Fives	0 violation	0 violation	0 violation	0 violation	0 violation
Bioavailability Score	0.55	0.55	0.55	0.55	0.55
GI absorption	High	High	High	High	High
BBB permeant	Yes	Yes	No	No	Yes

GI- Gastro Intestinal; BBB- Blood-Brain Barrier.

4. Discussion

High-affinity iron acquisition is mediated by siderophore-dependent pathways in the majority of pathogenic bacteria. Inhibition of siderophore-mediated iron acquisition is one of the promising strategies to control bacterial infections. Though inhibitors of siderophore biosynthesis and transport were reported earlier, no approved drugs are still available in the market [22-25]. Siderophores form tight and stable complexes with ferric iron [16]. Fe(III)-siderophore complexes are then transported into the bacterial cells, where the Fe^{3+} is converted into Fe^{2+} ion by enzymatic reactions [26, 27]. Enterobactin is a siderophore produced by most enteric pathogens, including *S. typhimurium* and *E. coli*. The biosynthesis of enterobactin has been well studied and reported by various researchers [28-30]. In the first step of the biosynthesis of enterobactin, chorismate is converted into isochorismate by the enzyme ICS

encoded by *entC* gene [31]. As this enzyme shares no homology with any of the human proteins, this was selected as one of the drug targets for this study.

Once the enterobactin binds to Fe^{3+} ion to form Fe(III)-enterobactin complex, it is transported into the bacterial cells. Recognition and incorporation of the ferric-enterobactin complex begin at an outer membrane protein receptor known as FepA [13, 15]. FepA was selected as another drug target for the current study as the inhibition of FepA mediated transport would stop the transport of Fe(III)-enterobactin complex into bacterial cells.

Bioprospecting of marine natural products has yielded a considerable number of drug candidates [32, 33]. Also, plant-derived substances have recently become of great interest owing to their versatile applications, including antibacterial, antiviral, and anti-inflammatory activities [34, 35, 36, 37]. For these reasons, herein number of marine and plant metabolites were screened for binding with the selected drug targets.

Analysis of the interaction of FepA with these compounds provides some insights into the binding site of FepA and the amino acids involved in the interaction. The amino acid residues Lys47, Leu57, Arg70, Arg108, Arg225, and Pro712, were found to be common in all the interactions. Among them, Lys47 and Pro712 are found to be interacting with all the five compounds from which we can interpret that these amino acids are important for the interactions with the ligand. Withanolide D was found to fit inside the β -barrel structure of FepA through which the Fe-enterobactin complex is reported to be transported [38].

The four amino acids, Ser215, Gly214, Gly361, and Ala303, make the active site of ICS [30]. All these four amino acids, along with four other amino acids (Arg347, Ala360, His276, and Lys380), were found to be interacting with the natural ligand of ICS. The compounds, laurediterpenol, isogranulatimide and plakorstatin B, interact with 6 out of 8 amino acids interacting with the natural ligand. Among these ligands, plakorstatin B is found to be binding exactly in the cavity where the natural ligand binds (Figure 7a and 7b). This shows that plakorstatin B can potentially be developed as a promising molecule that can inhibit enterobactin biosynthesis.

Three out of the 5 top binders of FepA, Withanolide D shows better ADME properties because the molecular weight of the other two compounds, daucosterol, and Bistramide, is greater than 500. Of all the top binders of ICS and the FepA, Withanolide D shows very good ADME properties, including high GI absorption, no BBB permeability, and a better bioavailability score, which indicates this compound could have the potential to be developed into a candidate drug to inhibit the biosynthesis of enterobactin.

5. Conclusions

Since antibiotic resistance is becoming a serious threat to humankind, developing novel alternative strategies to control bacterial pathogens is crucial. One of the novel strategies has been utilized in the current study. Marine and plant metabolites were screened to target enterobactin's biosynthesis and transport in *E. coli*, thereby interfering with iron sequestration. Out of 130 compounds screened, the top five binders for each drug target were identified as candidate drugs, which possess the potential to be developed into a drug. The top binder of FepA Withanolide D shows a good binding affinity (-12.61), found to bind exactly to the interior of the β -barrel structure of FepA, and possesses good ADME properties. This molecule can be regarded as a potential candidate molecule that can further be developed successfully into a drug.

Funding

Research grants to KS by Science and Engineering Research Board (SERB), New Delhi, India (SR/SO/HS-0248/2012; EMR/2016/003035) are gratefully acknowledged. MSCV was supported by a Research Fellowship from Kalasalingam Academy of Research and Education.

Acknowledgments

The authors thank the Kalasalingam Academy of Research and Education for the facilities provided.

Conflicts of Interest

The authors have no conflicts of interest.

References

1. Peterson, E.; Kaur P. Antibiotic Resistance Mechanisms in Bacteria: Relationships Between Resistance Determinants of Antibiotic Producers, Environmental Bacteria, and Clinical Pathogens. *Front Microbiol.* **2018**, *9*, 2928, <https://doi.org/10.3389/fmicb.2018.02928>.
2. <https://www.who.int/news-room/fact-sheets/detail/antimicrobial-resistance>. Accessed on December 10, **2021**.
3. Allen, R.C.; Popat, R.; Diggle, S.P.; Brown, S.P. Targeting virulence, can we make evolution proof drugs? *Nat. Rev. Microbiol.* **2014**, *12*, 300-308, <https://doi.org/10.1038/nrmicro3232>.
4. Rangel-Vega, A.; Bernstein, L.R.; Mandujano-Tinoco, E.A.; García-Contreras, S.J.; García-Contreras, R. Drug repurposing as an alternative for the treatment of recalcitrant bacterial infections. *Front. Microbiol.* **2015**, *6*, 282, <https://doi.org/10.3389/fmicb.2015.00282>.
5. Crosa, J.H. Genetics and molecular biology of siderophore-mediated iron transport in bacteria. *Microbiol. Rev.* **1989**, *53*, 517-530, <https://doi.org/10.1128/mr.53.4.517-530.1989>.
6. Aghajani, Z.; Rasooli, I.; Gargari, S.L.M. Protective potentials of a siderophore receptor against *Acinetobacter baumannii* infections. *Biointerface Res Appl Chem* **2019**, *9*, 3987-3995, <https://doi.org/10.33263/briac94.987995>.
7. Braun, V.; Killmann, H. Bacterial solutions to the iron-supply problem. *Trends Biochem. Sci.* **1999**, *24*, 104-109, [https://doi.org/10.1016/s0968-0004\(99\)01359-6](https://doi.org/10.1016/s0968-0004(99)01359-6).
8. Ferreras, J.A.; Ryu, J.S.; Di Lello, F.; Tan, D.S.; Quadri, L.E. Small-molecule inhibition of siderophore biosynthesis in *Mycobacterium tuberculosis* and *Yersinia pestis*. *Nat. Chem. Biol.* **2005**, *1*, 29-32, <https://doi.org/10.1038/nchembio706>.
9. Somu, R.V.; Boshoff, H.; Qiao, C.; Bennett, E.M.; Barry, C.E.; Aldrich, C.C. Rationally designed nucleoside antibiotics that inhibit siderophore biosynthesis of *Mycobacterium tuberculosis*. *J. Med. Chem.* **2006**, *49*, 31-34, <https://doi.org/10.1021/jm051060o>.
10. Pinto, L.J.; Moore, M.M. Screening method to identify inhibitors of siderophore biosynthesis in the opportunistic fungal pathogen, *Aspergillus fumigatus*. *Lett. Appl. Microbiol.* **2009**, *49*, 8-13, <https://doi.org/10.1111/j.1472-765x.2009.02582.x>.
11. Garénaux, A.; Caza, M.; Dozois, C.M. The Ins and Outs of siderophore mediated iron uptake by extra-intestinal pathogenic *Escherichia coli*. *Vet. Microbiol.* **2011**, *153*, 89-98, <https://doi.org/10.1016/j.vetmic.2011.05.023>.
12. Nagy, T.A.; Moreland, S.M.; Andrews-Polymenis, H.; Detweilera, C.S. The ferric enterobactin transporter Fep is required for persistent *Salmonella enterica* serovar typhimurium infection. *Infect. Immun.* **2013**, *81*, 4063-4070, <https://doi.org/10.1128/iai.00412-13>.
13. Usher, K.C.; Özkan, E.; Gardner, K.H.; Deisenhofer, J. The plug domain of FepA, a TonB-dependent transport protein from *Escherichia coli*, binds its siderophore in the absence of the transmembrane barrel domain. *PNAS* **2001**, *98*, 10676-10681, <https://doi.org/10.1073/pnas.181353398>.
14. Braun, V.; Hantke, K. Bacterial Iron Transport. In: *Molecular and Cellular Iron Transport*, Templeton, D.M., Ed., Marcel Dekker, New York **2002**, 395-426, <https://doi.org/10.1201/9780367800536>.

15. Raymond, K.N.; Dertz, E.A.; Kim, S.S. Enterobactin, An archetype for microbial iron transport. *PNAS* **2003**, *100*, 3584-3588, <https://doi.org/10.1073/pnas.0630018100>.
16. Khan, A.; Singh, P.; Srivastava, A. Synthesis, nature and utility of universal iron chelator – Siderophore: A review. *Microbiol Res* **2018**, *212–213*, 103-111, <https://doi.org/10.1016/j.micres.2017.10.012>.
17. Duke, J.A. *Handbook of phytochemical constituents of GRAS herbs and other economic plants*. CRC Press **1992**, Boca Raton, FL.
18. Haribalaganesh, R.; Rosy, J.C.; Rohita, S.; Aishwarya, C.; Brintha, S.; Rahul, S.; Sundar, K. Antiviral drugs against Ebola, A structure based virtual screening approach. *Indian J. Biotechnol.* **2018**, *17*, 176-184.
19. Morris, G.M.; Huey, R.; Lindstrom, W.; Sanner, M.F.; Belew, R.K.; Goodsell, D.S.; Olson, A.J. AutoDock4 and AutoDockTools4, automated docking with selective receptor flexibility. *J. Comput. Chem.* **2009**, *30*, 2785-2791, <https://doi.org/10.1002/jcc.21256>.
20. Cosconati, S.; Forli, S.; Perryman, A.L.; Harris, R.; Goodsell, D.S.; Olson, A. J. Virtual Screening with AutoDock: Theory and Practice. *Expert Opin Drug Discov.* **2010**, *5*, 597-607, <https://doi.org/10.1517/17460441.2010.484460>.
21. Parikesit, A.A.; Nurdiansyah, R.; Garrido, G. Natural Products repurposing of the H5N1-based lead compounds for the most fit inhibitors against 3C-like protease of SARS-CoV-2. *J Pharm Pharmacogn Res.* **2021**, *9*, 730-745,
22. Tillotson, G.S.; Theriault, N. New and alternative approaches to tackling antibiotic resistance. *F1000Prime Rep.* **2013**, *5*, 51, <https://doi.org/10.12703/p5-51>.
23. Sultan, I.; Rahman, S.; Jan, A.T.; Siddiqui, M.T.; Mondal, A.H.; Haq, Q.M.R. Antibiotics, Resistome and Resistance Mechanisms: A Bacterial Perspective. *Front Microbiol.* **2018**, *9*, 2066, <https://doi.org/10.3389/fmicb.2018.02066>.
24. Álvarez-Martínez, F.J.; Barrajon-Catalán, E.; Herranz-López, M.; Micol, V. Antibacterial plant compounds, extracts and essential oils: An updated review on their effects and putative mechanisms of action. *Phytomedicine* **2021**, *90*, 153626, <https://doi.org/10.1016/j.phymed.2021.153626>.
25. Chandra, H.; Bishnoi, P.; Yadav, A.; Patni, B.; Mishra, A.P.; Nautiyal, A.R. Antimicrobial resistance and the alternative resources with special emphasis on plant-based antimicrobials-A review. *Plants* **2017**, *6*, 16, <https://doi.org/10.3390/plants6020016>.
26. Stintzi, A.; Barnes, C.; Xu, J.; Raymond, K.N. Microbial iron transport via a siderophore shuttle: A membrane ion transport paradigm. *PNAS* **2000**, *97*, 10691-10696, <https://doi.org/10.1073/pnas.200318797>.
27. Page, M.G.P. The Role of Iron and Siderophores in Infection, and the Development of Siderophore Antibiotics. *Clin Infect Dis.* **2019**, *69*, S529-S537, <https://doi.org/10.1093/cid/ciz825>.
28. Crosa, J.H.; Walsh, C.T. Genetics and assembly line enzymology of siderophore biosynthesis in bacteria. *Microbiol. Mol. Biol. Rev.* **2002**, *66*, 223-249, <https://doi.org/10.1128/mmbr.66.2.223-249.2002>.
29. Saha, P.; Xiao, X.; Yeoh, B.S.; Chen, Q.; Katkere, B.; Kirimanjeswara, G.S.; Vijay-Kumar, M. The bacterial siderophore enterobactin confers survival advantage to *Salmonella* in macrophages. *Gut Microbes* **2019**, *10*, 412-423, <https://doi.org/10.1080/19490976.2018.1546519>.
30. Sora, V.M.; Meroni, G.; Martino, P.A.; Soggiu, A.; Bonizzi, L.; Zecconi, A. Extraintestinal Pathogenic *Escherichia coli*: Virulence Factors and Antibiotic Resistance. *Pathogens* **2021**, *10*, 1355, <https://doi.org/10.3390/pathogens10111355>.
31. Sridharan, S.; Howard, N.; Kerbarh, O.; Błaszczyk, M.; Abell, C.; Blundell, T.L. Crystal structure of *Escherichia coli* enterobactin-specific isochorismate synthase (EntC) bound to its reaction product isochorismate: implications for the enzyme mechanism and differential activity of chorismate-utilizing enzymes. *J. Mol. Biol.* **2010**, *397*, 290-300, <https://doi.org/10.1016/j.jmb.2010.01.019>.
32. Mishra, B.B.; Tiwari, V.K. Natural products, an evolving role in future drug discovery. *Eur. J. Med. Chem.* **2011**, *46*, 4769-4807, <https://doi.org/10.1016/j.ejmech.2011.07.057>.
33. Erba, E.; Bergamaschi, D.; Bassano, L.; Damia, G.; Ronzoni, S.; Faircloth, G.T.; D'Incalci, M. Ecteinascidin-743 (ET-743), a natural marine compound, with a unique mechanism of action. *Eur. J. Cancer* **2001**, *37*, 97-105, [https://doi.org/10.1016/s0959-8049\(00\)00357-9](https://doi.org/10.1016/s0959-8049(00)00357-9).
34. Najda, A.; Bains, A.; Chawla, P.; Kumar, A.; Balant, S.; Walasek-Janusz, M.; Wach, D.; Kaushik, R. Assessment of Anti-Inflammatory and Antimicrobial Potential of Ethanolic Extract of *Woodfordia fruticosa* Flowers: GC-MS Analysis. *Molecules* **2021**, *26*, 7193, <https://doi.org/10.3390/molecules26237193>.
35. Zhao, C.; Cao, Y.; Zhang, Z.; Nie, D.; Li, Y. Cinnamon and eucalyptus oils suppress the inflammation induced by Lipopolysaccharide In Vivo. *Molecules* **2021**, *26*, 7410, <https://doi.org/10.3390/molecules26237410>.

36. Noda, M.; Danshiitsoodol, N.; Sakaguchi, T.; Kanno, K.; Sugiyama, M. Exopolysaccharide produced by plant-derived *Lactobacillus plantarum* SN35N exhibits antiviral activity. *Biol Pharm Bull.* **2021**, *44*, 1886-1890, <https://doi.org/10.1248/bpb.b21-00517>.
37. Tian, L.; Wu, M.; Guo, W.; Li, H.; Gai, Z.; Gong, G. Evaluation of the membrane damage mechanism of chlorogenic acid against *Yersinia enterocolitica* and *Enterobacter sakazakii* and its application in the preservation of raw pork and skim milk. *Molecules* **2021**, *26*, 6748, <https://doi.org/10.3390/molecules26216748>.
38. Annamalai, R.; Jin, B.; Cao, Z.; Newton, S.M.; Klebba, P.E. Recognition of ferric catecholates by FepA. *J. Bacteriol.* **2004**, *186*, 3578-3589, <https://doi.org/10.1128/jb.186.11.3578-3589.2004>.